

Influence of Hot Multistage Drawing on Structure and Mechanical Properties of Nylon 6 Multifilament Yarn

Ruhollah Semnani Rahbar, Mohammad Reza Mohaddes Mojtahedi

Department of Textile Engineering, Amirkabir University of Technology, Tehran, IRAN

Correspondence to:

Mohammad Reza Mohaddes Mojtahedi email: mojtahed@aut.ac.ir

ABSTRACT

The effect of hot multistage drawing conditions on the structure and properties of nylon 6 fibers was investigated by varying second stage draw ratio. Total draw ratio was changed from 3.3 to 5.775 to clarify the structural changes in nylon 6 fiber at a broad range of draw ratio. The structural development of the fibers was studied with FTIR spectroscopy, differential scanning calorimetry (DSC), optical microscopy, and tensile testing. A continuous drop of the γ crystalline form content is observed as a function of draw ratio, in parallel with an increased content of α crystalline phase. The γ crystalline phase vanished completely at draw ratio of 4.62. Increasing draw ratio caused an increase in birefringence and no significant change occurred in crystallinity for the drawn nylon 6 fibers. Deformation behavior of drawn nylon 6 fibers has been explained in terms of applied thermal treatment and mechanical deformations which occurred in each step of multistage drawing.

KEYWORDS

Nylon 6 fiber, Hot multistage drawing, Crystallinity, Birefringence, Mechanical properties

INTRODUCTION

Nylon 6 is one of the most widely used engineering plastics and is also commercially produced in the form of fibers and films. Fiber morphology has been extensively studied for this polymer [1-5]. Based on various techniques, the investigations of these authors have revealed how complex the structural behavior of nylon 6 is related to processing parameters. Microstructural analysis and determination of the crystalline fraction is particularly complicated for nylon 6 because of existence of the α and γ crystal forms. The α crystalline form is most commonly observed at room temperature and can be obtained by slowly cooling from the melt state [6,7]. Crystal structure of the α crystalline phase is monoclinic, and consists of antiparallel extended zigzag chains. While the γ crystalline form is less stable with the hydrogen-bonding forming between parallel chains

and almost perpendicular to the carbon plane. The γ crystals of nylon 6 can be obtained by fiber spinning at high speed or through fast quenching from the melts. The γ crystalline phase can be converted to the α phase by phenol treatment [8] or by stretching [9] and the α to γ conversion can be achieved by iodine treatment [7,10].

The drawing process of the melt-spun nylon 6 fiber is often required in order to achieve the desired balance of fiber properties (e.g. modulus, tenacity, elongation). Important control parameters for fiber drawing are draw ratio, drawing temperature, drawing speed and the number of drawing stages. For apparel and carpet end-uses the nylon yarns are cold drawn, while in high tenacity industrial applications for tire cords and uses such as car seat belts, the yarns are drawn in hot multistage [11,12].

The effect of drawing on the structure and molecular orientation of nylon 6 fiber has been investigated by several researchers [3-5,13-23]. Microstructural changes that occur during drawing of nylon 6 fiber are usually characterized by various physical methods such as X-ray diffraction, differential scanning calorimetry (DSC), solid state NMR, polarized FTIR, density measurement, and optical microscope.

Among these, there are just few papers have been devoted to hot multistage drawing [3,4,13,18] and therefore the exact relationship between the drawing conditions, structural changes, and mechanical properties of drawn nylon 6 fiber upon hot multistage drawing have not yet been established. Therefore, the purpose of this paper is to study the structure-properties relation of the drawn nylon 6 fibers upon hot multistage drawing.

EXPERIMENTAL

Materials and Fiber Drawing

The experiments were performed with a low oriented polyamide 6 yarn (LOY) kindly supplied by Alyaf Co. (Iran). The undrawn multifilament yarn has a degree of polymerization of 110. The fully drawn of

this yarn is used routinely in the manufacture of fishnet. The yarn was 954 dtex, with 34 filaments of circular cross section. The drawing was carried out on an industrial Zinser draw-twisting machine (Germany), type 520-2.

A three-step drawing process was carried out on heated cylinders (godet roller) and hot plate by varying second-stage draw ratio. The drawing setup is shown schematically in *Figure 1*.

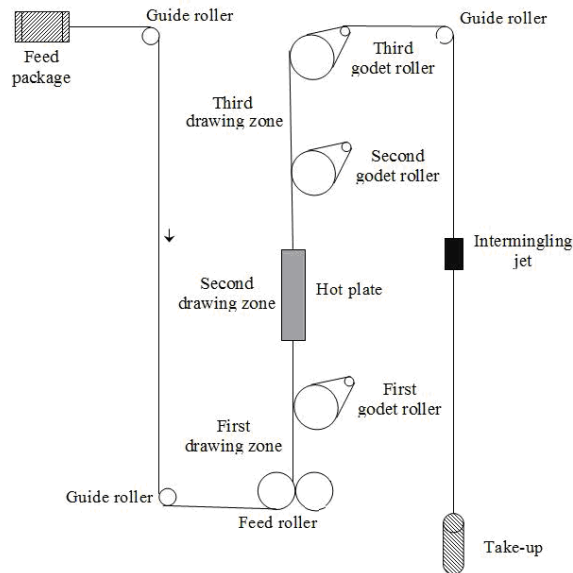


FIGURE 1. Schematic diagram of hot multistage drawing system

The different draw ratios of the drawn samples are shown in *Table I*. The total draw ratio is calculated by multiplication of the draw ratios employed.

TABLE I. Applied Draw Ratios in Different Stages of a Multistage Drawing Process

Sample	1 st stage draw ratio	2 nd stage draw ratio	3 rd stage draw ratio	Total draw ratio
1	1.1	2	1.5	3.3
2	1.1	2.2	1.5	3.63
3	1.1	2.4	1.5	3.96
4	1.1	2.6	1.5	4.29
5	1.1	2.8	1.5	4.62
6	1.1	3	1.5	4.95
7	1.1	3.2	1.5	5.28
8	1.1	3.3	1.5	5.445
9	1.1	3.5	1.5	5.775

The applied drawing conditions are listed in *Table II*. Number of wraps around each godet defines

the contact time of multifilament yarn with corresponding temperature. These conditions were deduced from preliminary experiments.

As can be seen in *Table I*, in the first stage of drawing, the draw ratio of 1.1 was constant in all experiments and acts like a pretension for straightening yarn filaments prior to main drawing stage (second stage). Then, according to elongation at break of undrawn yarn, the highest total draw ratio was calculated and forty drawn samples were produced in trial and error way to obtain the optimum conditions for producing samples. In this way, the draw ratio of 1.5 was selected for third stage in all experiments of drawing and the second stage of draw ratio was changed from 2 to 3.5.

Methods

Yarn linear density (expressed in dtex) was determined in accordance with ASTM D 1577-96. Mean values are the average of five measurements. The infrared spectra were recorded with a Nicolet Fourier Transform Spectrophotometer in transmission mode over the range of 4000-400 cm^{-1} using a resolution of 4 cm^{-1} . Bundles of filaments were used to collect the infrared spectra. At least 256 scans were obtained to achieve an adequate signal/noise ratio.

Differential scanning calorimetry (DSC) measurements were carried out on DSC 2010 machine (TA Instruments, New Castle, DE, USA) to examine the thermal behavior of multifilament yarns. Samples of 4-6 mg, which were cut from the fibers, were heated from room temperature to 240 $^{\circ}\text{C}$ at a heating rate of 10 $^{\circ}\text{C}/\text{min}$ under nitrogen atmosphere with the flow rate of 20 mL/min . The equipment was calibrated with indium ($T_m=156.6$ $^{\circ}\text{C}$ and $\Delta H=28.5$ J/g). From the heat of fusion, an apparent crystallinity (X) was determined by following equation:

$$X(\%) = \left(\frac{\Delta H}{\Delta H^*} \right) \times 100 \quad (1)$$

Where ΔH is the measured melting enthalpy and ΔH^* is the enthalpy of fusion of a 100% crystalline polyamide 6, it was taken as 167.2 J/g (40 cal/g) [23]. The filament birefringence was measured using a cross-polarized optical microscope (Carl Zeiss, Jena, Germany) and a Quartz compensator. The same microscope was used to measure the diameter of the fibers. Five specimens were chosen for this test and the reported data are statistical average of these measurements.

Stress-strain curves were obtained using an EMT-3050 tensile tester (Elima Co., Iran). The cross-head speed of 500 mm/min and pre-tension of 0.1 cN/tex were fixed for all measurements. The gauge lengths of 50 mm and 300 mm were employed for undrawn

sample and drawn samples, respectively. From stress-strain plots, the maximum load, initial modulus, specific work of rupture, tenacity and extension at breaking were evaluated. The reported values of all the mechanical properties have been averaged over at least twenty independent measurements.

TABLE II. The Operating Conditions in Drawing Experiments

Temperature of feeding roller (°C)	Temperature of first godet roller (°C)	Temperature of hot plate (°C)	Temperature of second godet roller (°C)	Temperature of third godet roller (°C)	Drawing speed (m/min)	Intermingling jet pressure (bar)	Spindle speed (rpm)
Room temperature	100	170	170	Room temperature	400	2	4800

RESULTS AND DISCUSSION

FTIR Analysis

Infrared spectra taken as a function of draw ratio in the frequency regions 1100-900 cm^{-1} is shown in Figure 2.

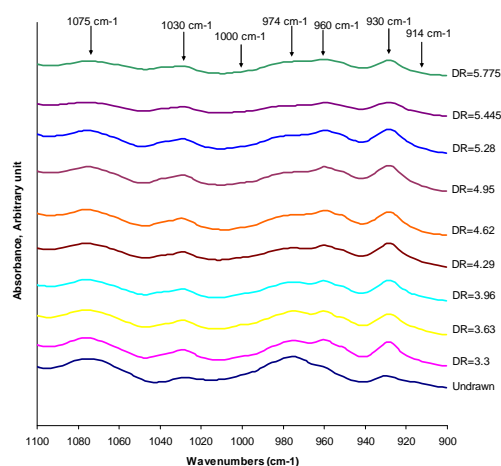


FIGURE 2. FTIR spectra (1100-900 cm^{-1}) of undrawn fiber and drawn fibers at different draw ratios.

According to numerous studies [3,16,22,24,25], this region with specific bands in FTIR spectra allows us to identify and follow the crystalline phase evolution induced thermally and mechanically in the nylon 6 fibers. In this spectrum, the peak intensities are shown to scale and are displaced vertically relative to each other for clarity of presentation. The band assignments for nylon-6 are well documented in the literatures [16,24].

As can be seen in Figure 2, for undrawn fiber, a strong band at 974 cm^{-1} and a weak band at 914 cm^{-1} showing this sample contains primarily of the γ -crystals. The peak at 930 cm^{-1} and barely visible shoulders at 960 cm^{-1} and 1030 cm^{-1} are indicating small amounts of the α -crystals exist in the undrawn

fiber [3,16,22]. After drawing, the bands at 930, 960 and 1030 cm^{-1} become sharper and stronger while the band at 914, 919, 974 and 1075 cm^{-1} becomes weaker and the 974 cm^{-1} band disappears completely in fiber drawn at draw ratio of DR=4.62. Moreover, the faint band at 1000 cm^{-1} appears in the drawn samples whereas this band does not exist in the undrawn fiber. Recently, Penel-Pierron *et al.* [25] reported that this band is absent in infrared spectra of nylon-6 pure amorphous and very high γ form content. Therefore, we can deduce from our spectra that the fraction of amorphous phase or the γ crystalline form decreases after hot multistage drawing.

The IR spectra of samples in the region of 1100-900 cm^{-1} indicate that the α -crystal phase generates during drawing and its developing occurs under three mechanisms including: thermal-induced crystallization and strain-induced crystallization of the amorphous phase and crystal morphology changes during hot multistage drawing (γ to α transformation). This finding is in agreement with previous observations [3,4,16,17]. It was proposed by Miyasaka and Makishima [9] that for γ to α transformation to occur, two conditions must be satisfied. First, there must be sufficient extension for the γ phase to untwist the chain around the amide group. Second, there has to be sufficient translation mobility of the change the stacking in the crystalline. Both mentioned conditions are present in the drawing process because of the applied heat and multistage drawing process and therefore the γ to α transformation occurs progressively.

Infrared spectroscopy has been used as an independent technique to measure crystallinity of polyamides [16,26] and other polymer [27,28] and also the α and γ crystalline phase content. Based on these FTIR spectra, a quantification of the crystalline phases as a function of draw ratio was made.

The 930 and 974 cm^{-1} peaks are used to determine the amounts of α and γ crystalline phases, respectively. A number of infrared bands have previously [3,16] been attributed to the amorphous bands of nylon 6, including bands at 1124 and 983 cm^{-1} . The band at 983 cm^{-1} is not an isolated band and overlaps strongly with the γ phase peak in drawn fibers and curve fitting is required to resolve this band. Therefore, we use the band at 1124 cm^{-1} for amorphous region.

Since the bands at 930 and 974 cm^{-1} are not isolated, it was necessary to deconvolute them in order to evaluate the contents of different crystalline forms present in nylon-6 fibers. *Figure 3* shows an example of the peak-fitting procedure for undrawn fiber and drawn fibers at low and high draw ratios.

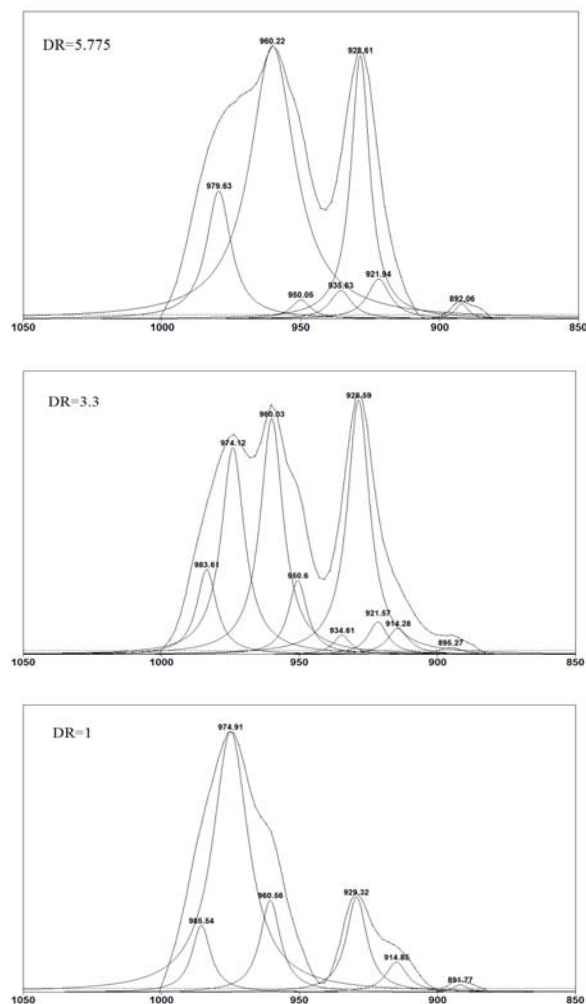


FIGURE 3. Curve fitting of the infrared spectra in the region of 1050-850 cm^{-1} for undrawn fiber and drawn fibers at draw ratios of 3.3 and 5.775

For peak fitting, each resulting plot of FTIR absorbance versus wavenumbers was modeled using

a Gaussian-Lorentzian peak shape with a linear baseline in the profile fitting program PeakFit™ (AISN Software, Inc.). The peak locations in wavenumbers were held constant, while the peak heights and widths were allowed to float. Prior to executing the auto-fit program, the height and breadths of each peak were adjusted manually in order to provide a reasonable starting point for the curve fitting to begin. Areas of the peaks obtained from the analysis were used to estimate the degree of crystallinity for each form. In general, agreement between model predictions and the raw data yielded coefficients of determinations, i.e. $R^2 > 0.98$.

The relative contribution of each crystalline form and amorphous phase in the samples with respect to total nylon-6 crystal phase content is reported as a function of draw ratio in *Figure 4*. For this purpose, it is necessary to normalize the entire spectra for sample thickness. This could be done by normalizing to the area between 750-600 cm^{-1} . We used the band at 930 cm^{-1} as a measure of the alpha phase, the band at 974 cm^{-1} as a measure of gamma phase, and the band at 1124 cm^{-1} as a measure of amorphous phase. We measured these peaks area, normalized to 100 before plotting the data in *Figure 4*. It should be noted that the α , γ and amorphous contents are calculated with the assumption of the constant absorbance coefficient for each absorbance band, and hence these are not absolute values.

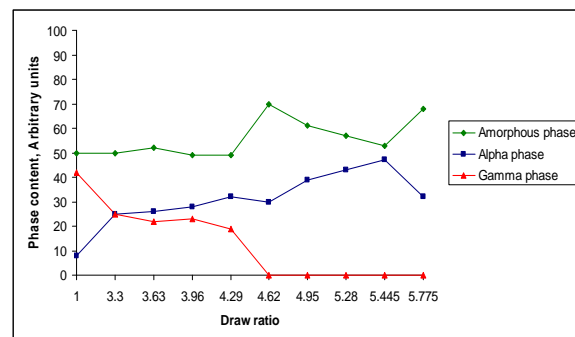


FIGURE 4. Relative changes in phase composition of nylon 6 fibers upon hot multistage drawing at different draw ratios

Up to draw ratio of 4.29, it is indicated that the total crystalline content and the amorphous content remain nearly constant while the content of the α crystalline form increases with draw ratio, and the opposite tendency is observed for the γ crystalline form. The data of *Figure 4* show that most of the γ crystalline phase is removed by a draw ratio of DR=3.3. This suggests that the hot multistage drawing is governed by stress-induced crystal-crystal transformation, i.e. the γ to α crystalline phase transformation while the

draw ratio is no more than DR=4.29. With further drawing, the γ crystals are destroyed at draw ratio of 4.62 and this causes the amorphous phase content increases drastically because the α crystalline phase content remains constant. Afterwards, the crystallization occurs in the form of α crystalline phase from amorphous phase. This behavior is quite similar to annealing of nylon 6 fiber in which the α crystalline phase produces primarily from the amorphous phase rather than from the γ crystalline phase [16]. In the highest applied draw ratio (DR=5.775), the amorphous phase content again increases which can be attributed to crystal destruction during hot multistage drawing at very high draw ratio. This is consisted with our DSC results in high draw ratio as will be shown later.

Thermal Analysis

The melting endotherms obtained for undrawn and drawn fibers at different draw ratios are shown in Figure 5. DSC thermograms of undrawn sample and drawn nylon 6 fibers displayed a single endothermic melting peak associated with the α crystalline form of nylon 6 in the 216-223 °C temperature range [22,25,29]. The baseline in the all DSC scans remains relatively flat almost until the main melting peak. Generally, the DSC thermograms of nylon 6 fiber containing both α and γ crystalline forms show a double endothermic peak in which the first peak appears about 10 °C lower than main melting peak. The first and second peaks correspond to the melting of the crystalline γ and α crystalline forms, respectively [6,30].

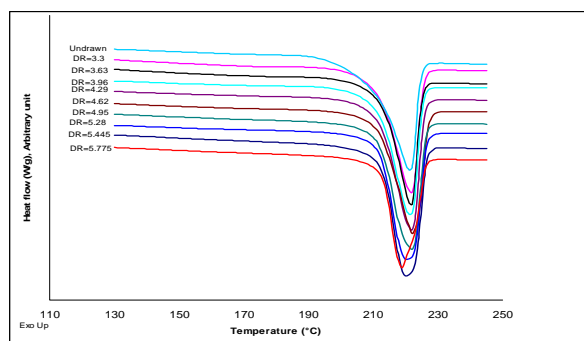


FIGURE 5. DSC thermograms of undrawn fiber and drawn fibers at different draw ratios

As indicated in FTIR results, the γ crystal form is present in the drawn fiber up to draw ratio of 4.62 Figure 4, but DSC curves show no sign of a melting peak at 210-215 °C characteristic of the thermally stable γ form. It seems that the relative amounts of γ crystalline phase in the drawn fibers are low and these crystals can not show a distinct melting peak in

DSC thermograms. Moreover, it may be supposed that the less stable γ crystals converted to more stable α crystal during heating in DSC experiment.

The main characteristics obtained from the DSC thermograms are summarized in Table III. It is apparent from Table III, the onset of melting and melting temperatures of drawn nylon 6 showed no considerable variation with increasing draw ratio. T_m was found to be 221.4 °C for undrawn fiber and 218.8 for fiber drawn at draw ratio of 5.775. The onset of melting in undrawn fiber (194 °C) is significantly lower than those of drawn fibers. This shows the presence of crystals with lower perfection, size and stability in undrawn fiber. The onset of melting temperature obtained here are lower than that previously reported in literatures in heat treated [31] or cold drawn nylon 6 fibers [32]. This may be arising from the existence of crystals with different sizes and perfections in nylon 6 fibers.

TABLE III. Thermal Property Characteristics of Undrawn Fiber and Drawn Fibers at Different Draw Ratios Obtained From DSC

Draw ratio	Onset of melting (°C)	Melting temperature (°C)	Heat of fusion (J/g)	Crystallinity (%)
1	194.1	221.4	57.19	34.20
3.3	206.4	221.7	66.30	39.65
3.63	208.1	221.5	58.30	34.86
3.96	206.7	221.4	68.44	40.93
4.29	206.5	221.8	68.45	40.93
4.62	207.9	221.7	68.83	41.16
4.95	208.8	221.8	70.41	42.11
5.28	209.4	220.3	71.64	42.84
5.445	208.2	220.0	73.26	43.81
5.775	210.2	218.8	68.87	41.19

The heat of fusion increases slowly with increasing draw ratio up to draw ratio of 5.445 and then decreases in fiber drawn at draw ratio of 5.775. There is also no significant difference in the heat of fusion of fibers drawn at draw ratios of 3.96 to 4.62. The difference between crystalline fractions of drawn fibers was not significant, but the crystallinity increases gradually with increasing draw ratio see (Table III). The undrawn fiber has the crystallinity (X_c %) of about 34.20 and this value reaches to 43.81 in fiber drawn at draw ratio of 5.445.

On this point, it should be underlined that in the course of drawing of semicrystalline polymers, such as nylon 6, the crystallinity can increase or decrease or even remains unchanged depending on several factors: the drawing conditions (draw ratio, draw rate, and temperature), the starting structure and the chemical nature and composition of the polymeric

system [16]. In our research, in spite of sufficient molecular mobility due to heat, there is a lack of significant change in heat of fusion, melting

temperature and crystallinity upon hot multistage drawing. This suggests that the crystalline region of nylon 6 fiber is not affected by draw ratio during hot multistage drawing.

Table IV. Filament Diameter and Birefringence Values of the Undrawn Fiber and Drawn Fibers at Different Draw Ratios

	Draw ratio									
	1	3.3	3.63	3.96	4.29	4.62	4.95	5.28	5.445	5.775
Filament diameter (μm)	51.0 (1.4)	35.0 (1.2)	32.0 (1.3)	31.6 (1.2)	30.0 (1.4)	29.5 (1.4)	27.5 (1.3)	27.5 (1.3)	26.6 (1.4)	26.5 (1.3)
Birefringence (Δn)	0.0090 (0.0010)	0.0437 (0.0011)	0.0450 (0.0020)	0.0491 (0.0012)	0.0551 (0.0010)	0.0558 (0.0013)	0.0581 (0.0011)	0.0593 (0.0005)	0.0600 (0.0011)	0.0616 (0.0002)

The numbers in parentheses are standard deviation

Although the molecular orientation increases strongly with draw ratio in hot multistage drawing (as will be shown later in *Table IV*), the molecular rearrangements occurring during the drawing process seem not to be enhancing the chances of neighboring chains falling into crystalline domain.

Birefringence

Filament diameter and birefringence of undrawn fiber and drawn fibers are presented in *Table IV*. Under three-stage drawing in hot condition, the fiber diameter decreased substantially at lower applied draw ratios and remains essentially unchanged at higher draw ratios ($\text{DR} > 4.95$). The diameter of filaments drawn at draw ratio of 5.775 is 26.5 μm . To examine the development of orientation during the spinning and drawing processes, the birefringence of nylon 6 fibers was measured. It is well known that drawing of polymeric fiber influences molecular orientation and, often, the degree of crystallinity [11]. It is evident from *Table IV* that the birefringence value increases with increasing draw ratio, but the negative deviation, i.e. decrease in the rate of birefringence increase with draw ratio, occurred at the higher draw ratio ($\text{DR} > 4.95$) and the birefringence reaches to a constant value. Similar observations have been made for nylon 6 fibers drawn in hot two-stage process [5]. In the hot drawing process, the temperature changes the molecular mobility due to input thermal energy and this decreases the resistance of the polymer network to deformation. Therefore, the efficiency of chain orientation during drawing of nylon 6 increases and gives rise to higher birefringence values. The birefringence values of nylon 6 fibers drawn in cold condition up to draw ratio of 4.5 show the same trend with increasing draw ratio, but their values do not reach to a saturated point [3,14]. It has been previously showed in FTIR discussion that the α phase is predominant in the fibers drawn at higher

draw ratio and γ phase content is negligible in these samples. Therefore, this trend in birefringence occurs in spite of the higher intrinsic birefringence (0.094) [33] value reported for α crystals than γ crystals (0.066) [33]. It seems that the intermolecular linkage broken down in the fibers drawn at $\text{DR} > 4.95$, and consequently molecular chains might slip past one another and flow individually, exhibiting a large deformation without inducing any significant molecular orientation.

Tensile Properties

Figure 6 shows the tensile stress-strain curves for undrawn multifilament yarn and drawn samples recorded at room temperature.

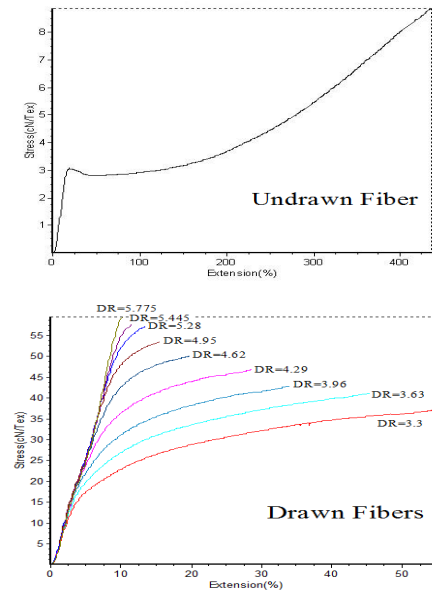


FIGURE 6. Stress-strain curves of undrawn fiber and drawn fibers at different draw ratios

The stress-strain curve for undrawn fiber shows a typical behavior of low oriented nylon 6 fiber. That is, the tensile stress initially increased rapidly,

followed by a neck formation, and then increased gradually to a maximum specific stress of about 8.3 cN/tex. However, no necking appeared for the drawn fibers at different draw ratios and they only showed homogeneous deformation behavior. The shapes of the curves are distinctly different at different draw ratios. At the lowest draw ratio (DR=3.3), a short linear portion is seen at low strain values. As the draw ratio goes higher, this linear region tends to become longer and at higher draw ratio (DR>5.28), the entire curve is almost linear.

The mechanical properties of these samples are summarized in *Table V*. The fiber drawing at three steps was found to be effective in the improvement of the mechanical properties. For a low draw ratio (DR=3.3), the initial modulus and tenacity of the drawn fibers are 314.1 cN/tex and 21.9 cN/tex, respectively. For the highest draw ratio (DR=5.775), the initial modulus is 650.4 cN/tex (i.e. an increase of

107%) and the tenacity reaches 59.6 cN/tex (i.e. an increase of 172.1%). At the same time, the elongation at break decreases strongly when the draw ratio increases. At a low draw ratio (DR=3.3), the elongation at break is 55.7% and falls down to 10.1% in fibers drawn at draw ratio of 5.775 (i.e. a decrease of 82%). These results reflect the observed differences in orientation of the filaments as measured by the birefringence values see *Table IV*. Work of rupture is defined as the area under the stress–strain curve. The specific work of rupture has the highest value of 20 cN/tex in the undrawn fiber, while the lowest value of 2.1 cN/tex achieved at the highest draw ratio. It is interesting to note that the sensitivity of the work of rupture to elongation at break in the drawn fibers is higher than to the specific stress.

TABLE V. Tensile Properties of Undrawn Fiber and Drawn Fibers at Different Draw Ratios

Draw ratio	Linear density (dtex)	Tenacity (cN/tex)	Elongation at break (%)	Initial modulus (cN/tex)	Specific work of rupture (cN/tex)
1	954 (15.1)	8.3 (0.8)	453.7 (24.5)	22.1 (1.5)	20.0 (1.8)
3.3	360 (0.8)	21.9 (1.3)	55.7 (7.5)	314.1 (13.4)	9.5 (1.5)
3.63	330 (0.9)	26.3 (0.7)	45.5 (4.1)	378.2 (14.1)	9.2 (1.0)
3.96	302 (0.9)	29.9 (0.8)	34.0 (4.3)	433.4 (18.9)	7.8 (1.1)
4.29	280 (0.7)	35.2 (1.6)	28.7 (3.1)	472.8 (10.3)	7.7 (1.1)
4.62	262 (0.8)	40.3 (1.2)	19.8 (2.7)	537.4 (23.9)	5.7 (1.1)
4.95	246 (0.8)	45.9 (1.2)	15.5 (1.9)	578.5 (26.9)	4.6 (0.9)
5.28	233 (1.0)	51.7 (1.7)	13.5 (2.4)	580.3 (13.8)	4.1 (1.2)
5.445	224 (0.8)	54.3 (1.6)	11.5 (1.6)	634.3 (24.6)	3.3 (0.8)
5.775	221 (0.9)	59.6 (2.4)	10.1 (0.9)	650.4 (20.6)	2.1 (0.5)

The numbers in parentheses are standard deviation

In spite of absence of significant change or even decrease in drawn fibers crystallinity (*Table III* in Thermal analysis discussion), the improvement in tenacity and initial modulus obtained for fiber drawn at draw ratio of 5.775, thus indicates that the orientation is responsible for the improvement of these properties.

On the other hand, as demonstrated in FTIR discussion, during hot multistage drawing the γ crystals converted to the α crystals and these newly formed α crystals are less ductile and deformable

than the original γ crystals, having lower H-bonded intersheet distances and therefore has higher inherent strength [22,30]. So, the nylon 6 fibers were drawn at higher draw ratios required more stress for crystal slip deformation and breaking and have less extensibility during tensile testing.

Deformation Behavior

In hot multistage drawing, the structure of drawn fibers forms gradually and at each stage, heat input and applied tension and stress have a special effect on the resultant drawn fibers. In our applied drawing

process, the first stage was performed at cold condition while drawing in second and third stage was carried out in hot conditions.

The first stage drawing in hot multistage drawing was performed on the nylon 6 fiber which already contained high γ crystalline phase content and low orientated region as shown in *Figure 2* and *Table IV*, respectively. Whereas, second and third step processes started from a partially drawn yarn with higher orientation. We supposed that the temperature on the first godet roller and also induced strain cause orientation of the molecular segments in the amorphous region at first stage of drawing, whereas the temperature on the hot plate and second godet roller and higher applied draw ratio in this stage, mainly affect on crystalline structure of fibers and amplified strain induced crystallization. Besides, it was demonstrated previously [16] that the thermally induces crystallization of nylon 6 starts to occur above 160 °C. So it seems that the most fraction of applied heat on first godet roller consumes for γ to α crystalline form transformation and after passing the moving fibers over the hot plate and second godet roller, thermally induced crystallization begins and also the mentioned crystalline phase transformation takes place more. The structural changes in third stage of drawing are strongly depended on the as-formed structure in previous stages. It seems that in this stage, the fixation of new more oriented state of the macromolecules which are formed in first and second stages and also increase in fiber orientation occurs. It should be noted that the first and third stages of drawing induce minor structural changes as compared to second stage effects. It can say although multistage drawing and applied heat amplified the transformation of γ to α phase; it seems that draw ratio is a more important variable than drawing temperature in controlling the γ to α crystalline phase transformation.

CONCLUSIONS

By considering the effect of hot multistage drawing on the structure and properties of nylon 6 fiber, we are able to draw the following conclusions. Multifilament yarn drawing conditions that comprise thermal treatment and mechanical deformations cause significant change in filament structure.

The hot multistage drawing of nylon 6 fibers involved both the γ to α crystalline phase transformation and crystallization of the amorphous phase into the α crystalline form. Most of the transformation occurs between a draw ratio of 1 and 3.3. With considering the FTIR and DSC results, it may be concluded that the γ to α crystalline phase

transformation is most probable to occur during hot multistage drawing and crystallization of the amorphous phase is significant after a specific draw ratio. The results show that the nylon 6 fiber has a low potential for additional crystallization with increasing draw ratio during hot multistage drawing. The birefringence increases linearly up to high draw ratio and this shows that the drawing is effective in extending chain molecules without relaxation of the orientation resulted from a chain slippage. The cooperation of heating and tension is very effective to form a favorable superstructure for improving tensile properties.

ACKNOWLEDGMENTS

The authors thank Alyaf Co. for supplying the undrawn yarn used in this study. The authors are also indebted to Dr. M. A. Tavanaie for arranging to produce the drawn samples. Prof. N. S. Murthy (University of Vermont) and Dr. N. Vasanthan (TRI/Princeton) are gratefully acknowledged for fruitful discussions on the interpretation of FTIR curves.

REFERENCES

- [1] Heuvel H. M.; Huisman R; *Journal of Applied Polymer Science* 1981, 26, 713-732.
- [2] Murthy N. S.; Curran S. A.; Aharoni S. M.; Minor H.; *Macromolecules* 1991, 24, 3215-3220.
- [3] Murthy N. S.; Bray R. G.; Correale S. T.; Moore R. F. A.; *Polymer* 1995, 36, 3863-3873.
- [4] Schreiber R.; Veeman W. S.; Gabriëls W.; Arnauts J.; *Macromolecules* 1999, 32, 4647-4657.
- [5] Penning J. P.; Ruiten J. van; Brouwer R.; Gabriëls W.; *Polymer* 2003, 44, 5869-5876.
- [6] Illers H. K.; Haberkorn H.; Siamk P.; *Die Makromolekulare Chemie* 1972, 158, 285-311.
- [7] Parker J. P.; Lindenmeyer P. H.; *Journal of Applied Polymer Science* 1977, 21, 821-837.
- [8] Hoashi K.; Andrews R. D.; *Journal of Polymer Science: Polymer Symposium* 1972, 38, 387-404.
- [9] Miyasaka K.; Makishima K.; *Journal of Polymer Science Part A-1: Polymer Chemistry* 1967, 5, 3017-3027.
- [10] Murthy N. S.; *Polymer Communication* 1991, 32, 301-305.
- [11] Salem D. R.; In *Structure formation in polymeric fibers*; Salem D. R.; Ed., Hanser Publishers: Munich, 2000, 118-184.

- [12] Morton W. E.; Hearle J. W. S.; *Physical properties of textile fibers*, 4th edn. Woodhead Publishing: London, 2008.
- [13] Song J. W.; Abhiraman A. S.; Richards A. P.; *Journal of Applied Polymer Science* 1982, 27, 2369-2375.
- [14] Prevorsek D. C.; Harget P. J.; Sharma R. K.; Reimschuessel A. C.; *Journal of Macromolecular Science Part B: Physics* 1973, 8, 127-156..
- [15] Fouda I. M.; El-Sharkawy F. M.; *Journal of Applied Polymer Science* 2004, 94, 287-295.
- [16] Vasanthan N.; Salem D. R.; *Journal of Polymer Science Part B: Polymer Physics* 2001, 39, 536-547.
- [17] Vasanthan N.; *Journal of Polymer Science Part B: Polymer Physics* 2003, 41, 2870-2877.
- [18] Butler R. H.; Prevorsek D. C.; Kwon Y. D.; *Polymer Engineering and Science* 1982, 22, 329-344.
- [19] Misra A.; Dutta B.; Prasad V. K.; *Journal of Applied Polymer Science* 1986, 31, 441-455.
- [20] Gianchandani J.; Spruiell J. E.; Clark E. S.; *Journal of Applied Polymer Science* 1982, 27, 3527-3551.
- [21] Penel-Pierron L.; Séguéla R.; Lefebvre J-M.; Miri V.; Depecker C.; Jutigny M.; Pabiot J.; *Journal of Polymer Science Part B: Polymer Physics* 2001, 39, 1224-1236.
- [22] Na B.; Lv R.; Tian N.; Xu W.; Li Z.; Fu Q.; *Journal of Polymer Science Part B: Polymer Physics* 2009, 47, 898-902.
- [23] Kunugi T.; Chida K.; Suzuki A.; *Journal of Applied Polymer Science* 1998, 67, 1993-2000.
- [24] Loo L. S.; Gleason K. K.; *Macromolecules* 2003, 36, 2587-2590.
- [25] Penel-Pierron L.; Depecker C.; Séguéla R.; Lefebvre J-M.; *Journal of Polymer Science Part B: Polymer Physics* 2001, 39, 484-495.
- [26] Vasanthan N.; Salem D. R.; *Journal of Polymer Science Part B: Polymer Physics* 2000, 38, 516-524.
- [27] Vasanthan N.; Ly O.; *Polymer Degradation and Stability* 2009, 94, 1364-1372.
- [28] Chuah H. H.; *Macromolecules* 2001, 34, 6985-6993.
- [29] Khanna Y. P.; Kuhn W. P.; *Journal of Polymer Science Part B: Polymer Physics* 1997, 35, 2219-2231.
- [30] Bureau M. N.; Denaulty J.; Cole K. C.; Enright G. D.; *Polymer Engineering and Science* 2002, 42, 1897-1906.
- [31] Correale S. T.; Murthy N. S.; *Journal of Applied Polymer Science* 2006, 101, 447-454.
- [32] Vasanthan N.; *Journal of Applied Polymer Science* 2003, 90, 772-775.
- [33] Murase S.; Matsuda T.; Hirami M.; *Macromolecular Materials and Engineering* 2000, 281, 48-51.

AUTHORS' ADDRESSES

Ruhollah Semnani Rahbar
Mohammad Reza
Mohaddes Mojtahedi
 Amirkabir University of Technology
 Department of Textile Engineering
 P.O. Box 15875-4413
 Tehran, IRAN